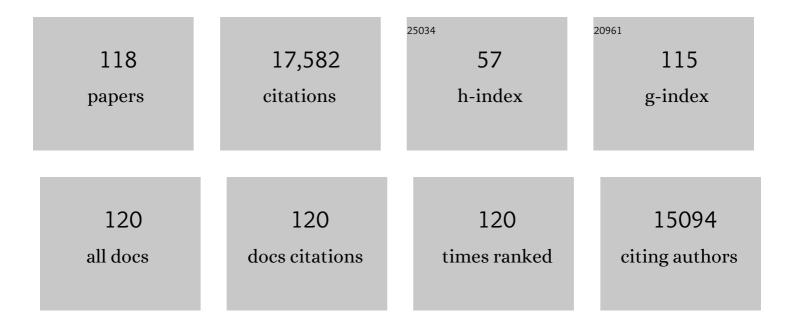
List of Publications by Year in descending order

Source: https://exaly.com/author-pdf/9148019/publications.pdf Version: 2024-02-01



CVF WON HAN

| # | Article | IF | CITATIONS |
|----|--|------|-----------|
| 1 | Structure of the Human Dopamine D3 Receptor in Complex with a D2/D3 Selective Antagonist. Science, 2010, 330, 1091-1095. | 12.6 | 1,034 |
| 2 | Structural Basis for Allosteric Regulation of GPCRs by Sodium Ions. Science, 2012, 337, 232-236. | 12.6 | 860 |
| 3 | Structure of the human \hat{I}^{e} -opioid receptor in complex with JDTic. Nature, 2012, 485, 327-332. | 27.8 | 797 |
| 4 | Structure of an Agonist-Bound Human A _{2A} Adenosine Receptor. Science, 2011, 332, 322-327. | 12.6 | 783 |
| 5 | Structure of the human histamine H1 receptor complex with doxepin. Nature, 2011, 475, 65-70. | 27.8 | 727 |
| 6 | Crystal structure of rhodopsin bound to arrestin by femtosecond X-ray laser. Nature, 2015, 523, 561-567. | 27.8 | 683 |
| 7 | Structure of the CCR5 Chemokine Receptor–HIV Entry Inhibitor Maraviroc Complex. Science, 2013, 341, 1387-1390. | 12.6 | 606 |
| 8 | Crystal Structure of a Lipid G Protein–Coupled Receptor. Science, 2012, 335, 851-855. | 12.6 | 600 |
| 9 | Structural Features for Functional Selectivity at Serotonin Receptors. Science, 2013, 340, 615-619. | 12.6 | 600 |
| 10 | Lipidic cubic phase injector facilitates membrane protein serial femtosecond crystallography. Nature Communications, 2014, 5, 3309. | 12.8 | 505 |
| 11 | Structure of a Class C GPCR Metabotropic Glutamate Receptor 1 Bound to an Allosteric Modulator. Science, 2014, 344, 58-64. | 12.6 | 476 |
| 12 | Crystal Structure of the Human Cannabinoid Receptor CB1. Cell, 2016, 167, 750-762.e14. | 28.9 | 468 |
| 13 | Structural Basis for Molecular Recognition at Serotonin Receptors. Science, 2013, 340, 610-614. | 12.6 | 454 |
| 14 | Serial Femtosecond Crystallography of G Protein–Coupled Receptors. Science, 2013, 342, 1521-1524. | 12.6 | 424 |
| 15 | Structure of the human smoothened receptor bound to an antitumour agent. Nature, 2013, 497, 338-343. | 27.8 | 415 |
| 16 | Crystal structures of agonist-bound human cannabinoid receptor CB1. Nature, 2017, 547, 468-471. | 27.8 | 379 |
| 17 | Structure of the human glucagon class B G-protein-coupled receptor. Nature, 2013, 499, 444-449. | 27.8 | 352 |
| 18 | Structure of the human P2Y12 receptor in complex with an antithrombotic drug. Nature, 2014, 509, 115-118. | 27.8 | 330 |

| # | Article | IF | CITATIONS |
|----|---|------|-----------|
| 19 | Crystal structure of the chemokine receptor CXCR4 in complex with a viral chemokine. Science, 2015, 347, 1117-1122. | 12.6 | 325 |
| 20 | Structure of the Angiotensin Receptor Revealed by Serial Femtosecond Crystallography. Cell, 2015, 161, 833-844. | 28.9 | 315 |
| 21 | Two disparate ligand-binding sites in the human P2Y1 receptor. Nature, 2015, 520, 317-321. | 27.8 | 305 |
| 22 | Structure of the Nanobody-Stabilized Active State of the Kappa Opioid Receptor. Cell, 2018, 172, 55-67.e15. | 28.9 | 299 |
| 23 | Agonist-bound structure of the human P2Y12 receptor. Nature, 2014, 509, 119-122. | 27.8 | 279 |
| 24 | Crystal Structure of the Human Cannabinoid Receptor CB2. Cell, 2019, 176, 459-467.e13. | 28.9 | 268 |
| 25 | Structure of CC chemokine receptor 2 with orthosteric and allosteric antagonists. Nature, 2016, 540, 458-461. | 27.8 | 220 |
| 26 | Structural basis for Smoothened receptor modulation and chemoresistance to anticancer drugs. Nature Communications, 2014, 5, 4355. | 12.8 | 208 |
| 27 | Human GLP-1 receptor transmembrane domain structure in complex with allosteric modulators. Nature, 2017, 546, 312-315. | 27.8 | 192 |
| 28 | 5-HT2C Receptor Structures Reveal the Structural Basis of GPCR Polypharmacology. Cell, 2018, 172, 719-730.e14. | 28.9 | 185 |
| 29 | Structure of the full-length glucagon class B G-protein-coupled receptor. Nature, 2017, 546, 259-264. | 27.8 | 179 |
| 30 | Structural basis of non-specific lipid binding in maize lipid-transfer protein complexes revealed by high-resolution X-ray crystallography1 1Edited by D. Rees. Journal of Molecular Biology, 2001, 308, 263-278. | 4.2 | 175 |
| 31 | Structural basis for selectivity and diversity in angiotensin II receptors. Nature, 2017, 544, 327-332. | 27.8 | 174 |
| 32 | Allosteric Coupling of Drug Binding and Intracellular Signaling in the A2A Adenosine Receptor. Cell, 2018, 172, 68-80.e12. | 28.9 | 173 |
| 33 | Crystal Structure of Antagonist Bound Human Lysophosphatidic Acid Receptor 1. Cell, 2015, 161, 1633-1643. | 28.9 | 169 |
| 34 | Structural basis for bifunctional peptide recognition at human δ-opioid receptor. Nature Structural and Molecular Biology, 2015, 22, 265-268. | 8.2 | 151 |
| 35 | Structure of CC Chemokine Receptor 5 with a Potent Chemokine Antagonist Reveals Mechanisms of Chemokine Recognition and Molecular Mimicry by HIV. Immunity, 2017, 46, 1005-1017.e5. | 14.3 | 148 |
| 36 | Structural Basis for Ligand Recognition and Functional Selectivity at Angiotensin Receptor. Journal of Biological Chemistry, 2015, 290, 29127-29139. | 3.4 | 145 |

| # | Article | IF | CITATIONS |
|----|---|------|-----------|
| 37 | Structural basis of ligand recognition at the human MT1 melatonin receptor. Nature, 2019, 569, 284-288. | 27.8 | 140 |
| 38 | Structural Connection between Activation Microswitch and Allosteric Sodium Site in GPCR Signaling. Structure, 2018, 26, 259-269.e5. | 3.3 | 134 |
| 39 | The Role of a Sodium Ion Binding Site in the Allosteric Modulation of the A2A Adenosine G Protein-Coupled Receptor. Structure, 2013, 21, 2175-2185. | 3.3 | 118 |
| 40 | Defining GC-specificity in the minor groove: side-by-side binding of the di-imidazole lexitropsin to C-A-T-G-C-C-A-T-G. Structure, 1997, 5, 1033-1046. | 3.3 | 109 |
| 41 | XFEL structures of the human MT2 melatonin receptor reveal the basis of subtype selectivity. Nature, 2019, 569, 289-292. | 27.8 | 106 |
| 42 | Native phasing of x-ray free-electron laser data for a G protein–coupled receptor. Science Advances, 2016, 2, e1600292. | 10.3 | 97 |
| 43 | Structural Basis for Apelin Control of the Human Apelin Receptor. Structure, 2017, 25, 858-866.e4. | 3.3 | 96 |
| 44 | Structural basis of the activation of a metabotropic GABA receptor. Nature, 2020, 584, 298-303. | 27.8 | 92 |
| 45 | Determination of the melanocortin-4 receptor structure identifies Ca ²⁺ as a cofactor for ligand binding. Science, 2020, 368, 428-433. | 12.6 | 89 |
| 46 | Structural and Biophysical Characterization of the EphB4·EphrinB2 Protein-Protein Interaction and Receptor Specificity. Journal of Biological Chemistry, 2006, 281, 28185-28192. | 3.4 | 87 |
| 47 | Full-length human GLP-1 receptor structure without orthosteric ligands. Nature Communications, 2020, 11, 1272. | 12.8 | 83 |
| 48 | Crystal structures of two novel dyeâ€decolorizing peroxidases reveal a βâ€barrel fold with a conserved hemeâ€binding motif. Proteins: Structure, Function and Bioinformatics, 2007, 69, 223-233. | 2.6 | 81 |
| 49 | Crystal structure of a multi-domain human smoothened receptor in complex with a super stabilizing ligand. Nature Communications, 2017, 8, 15383. | 12.8 | 81 |
| 50 | Elucidating the active δ-opioid receptor crystal structure with peptide and small-molecule agonists. Science Advances, 2019, 5, eaax9115. | 10.3 | 81 |
| 51 | Crystal structure of the Frizzled 4 receptor in a ligand-free state. Nature, 2018, 560, 666-670. | 27.8 | 77 |
| 52 | Structural Basis of Murein Peptide Specificity of a Î ³ -D-Glutamyl-L-Diamino Acid Endopeptidase. Structure, 2009, 17, 303-313. | 3.3 | 73 |
| 53 | Structure-based mechanism of cysteinyl leukotriene receptor inhibition by antiasthmatic drugs. Science Advances, 2019, 5, eaax2518. | 10.3 | 71 |
| 54 | Crystal structure of the global regulatory protein CsrA from Pseudomonas putida at 2.05 Ã resolution reveals a new fold. Proteins: Structure, Function and Bioinformatics, 2005, 61, 449-453. | 2.6 | 69 |

| # | Article | IF | CITATIONS |
|----|--|------|-----------|
| 55 | Exploring the potential impact of an expanded genetic code on protein function. Proceedings of the National Academy of Sciences of the United States of America, 2015, 112, 6961-6966. | 7.1 | 69 |
| 56 | Identification and structural characterization of heme binding in a novel dyeâ€decolorizing peroxidase, TyrA. Proteins: Structure, Function and Bioinformatics, 2007, 69, 234-243. | 2.6 | 67 |
| 57 | The Importance of Ligand-Receptor Conformational Pairs in Stabilization: Spotlight on the N/OFQ G Protein-Coupled Receptor. Structure, 2015, 23, 2291-2299. | 3.3 | 64 |
| 58 | Structural basis for signal recognition and transduction by platelet-activating-factor receptor. Nature Structural and Molecular Biology, 2018, 25, 488-495. | 8.2 | 58 |
| 59 | Structural basis of ligand binding modes at the human formyl peptide receptor 2. Nature Communications, 2020, 11, 1208. | 12.8 | 58 |
| 60 | Structure-based chemical modification strategy for enzyme replacement treatment of phenylketonuria. Molecular Genetics and Metabolism, 2005, 86, 134-140. | 1.1 | 57 |
| 61 | Structural insights into the extracellular recognition of the human serotonin 2B receptor by an antibody. Proceedings of the National Academy of Sciences of the United States of America, 2017, 114, 8223-8228. | 7.1 | 54 |
| 62 | Toward G protein-coupled receptor structure-based drug design using X-ray lasers. IUCrJ, 2019, 6, 1106-1119. | 2.2 | 53 |
| 63 | Metal ions and phosphate binding in the H-N-H motif: Crystal structures of the nuclease domain of ColE7/Im7 in complex with a phosphate ion and different divalent metal ions. Protein Science, 2009, 11, 2947-2957. | 7.6 | 51 |
| 64 | X-ray laser diffraction for structure determination of the rhodopsin-arrestin complex. Scientific Data, 2016, 3, 160021. | 5.3 | 51 |
| 65 | Structure of a DNA analog of the primer for HIV-1 RT second strand synthesis 1 1Edited by P. E. Wright. Journal of Molecular Biology, 1997, 269, 811-826. | 4.2 | 49 |
| 66 | Structural basis of ligand selectivity and disease mutations in cysteinyl leukotriene receptors. Nature Communications, 2019, 10, 5573. | 12.8 | 47 |
| 67 | Functional and structural characterization of a thermostable acetyl esterase from <i>Thermotoga maritima</i> . Proteins: Structure, Function and Bioinformatics, 2012, 80, 1545-1559. | 2.6 | 46 |
| 68 | An Unusual Sugar Conformation in the Structure of an RNA/DNA Decamer of the Polypurine Tract May Affect Recognition by RNase H. Journal of Molecular Biology, 2003, 334, 653-665. | 4.2 | 42 |
| 69 | Crystal Structure of the First Eubacterial Mre11 Nuclease Reveals Novel Features that May Discriminate Substrates During DNA Repair. Journal of Molecular Biology, 2010, 397, 647-663. | 4.2 | 41 |
| 70 | Crystal structure of soluble MD-1 and its interaction with lipid IVa. Proceedings of the National Academy of Sciences of the United States of America, 2010, 107, 10990-10995. | 7.1 | 37 |
| 71 | Trapping a transition state in a computationally designed protein bottle. Science, 2015, 347, 863-867. | 12.6 | 36 |
| 72 | The Structure of a Eukaryotic Nicotinic Acid Phosphoribosyltransferase Reveals Structural Heterogeneity among Type II PRTases. Structure, 2005, 13, 1385-1396. | 3.3 | 35 |

| # | Article | IF | CITATIONS |
|----|---|------|-----------|
| 73 | Bacterial Pleckstrin Homology Domains: A Prokaryotic Origin for the PH Domain. Journal of Molecular Biology, 2010, 396, 31-46. | 4.2 | 32 |
| 74 | Crystal structure of misoprostol bound to the labor inducer prostaglandin E2 receptor. Nature Chemical Biology, 2019, 15, 11-17. | 8.0 | 32 |
| 75 | Structural Basis of the Diversity of Adrenergic Receptors. Cell Reports, 2019, 29, 2929-2935.e4. | 6.4 | 30 |
| 76 | Crystal structure of acireductone dioxygenase (ARD) from Mus musculus at 2.06 Ã resolution. Proteins: Structure, Function and Bioinformatics, 2006, 64, 808-813. | 2.6 | 28 |
| 77 | Structural and Functional Characterizations of SsgB, a Conserved Activator of Developmental Cell Division in Morphologically Complex Actinomycetes. Journal of Biological Chemistry, 2009, 284, 25268-25279. | 3.4 | 23 |
| 78 | Crystal structure of the Fic (Filamentation induced by cAMP) family protein SO4266 (gi 24375750) from <i>Shewanella oneidensis</i> MRâ€I at 1.6 Ă resolution. Proteins: Structure, Function and Bioinformatics, 2009, 75, 264-271. | 2.6 | 23 |
| 79 | Structural insights into the molecular mechanisms of myasthenia gravis and their therapeutic implications. ELife, 2017, 6, . | 6.0 | 22 |
| 80 | Crystal Structure of a Voltage-gated K+ Channel Pore Module in a Closed State in Lipid Membranes. Journal of Biological Chemistry, 2012, 287, 43063-43070. | 3.4 | 21 |
| 81 | Generation of an Orthogonal Protein–Protein Interface with a Noncanonical Amino Acid. Journal of the American Chemical Society, 2017, 139, 5728-5731. | 13.7 | 18 |
| 82 | Crystal structure of an RNA{middle dot}DNA hybrid reveals intermolecular intercalation: Dimer formation by base-pair swapping. Proceedings of the National Academy of Sciences of the United States of America, 2003, 100, 9214-9219. | 7.1 | 17 |
| 83 | Molecular Mechanism for Ligand Recognition and Subtype Selectivity of α2C Adrenergic Receptor. Cell Reports, 2019, 29, 2936-2943.e4. | 6.4 | 17 |
| 84 | Crystal structure of S-adenosylmethionine:tRNA ribosyltransferase-isomerase (QueA) from Thermotoga maritima at 2.0 A resolution reveals a new fold. Proteins: Structure, Function and Bioinformatics, 2005, 59, 869-874. | 2.6 | 16 |
| 85 | A Structural Basis for the Regulatory Inactivation of DnaA. Journal of Molecular Biology, 2009, 385, 368-380. | 4.2 | 15 |
| 86 | A Single Reactive Noncanonical Amino Acid Is Able to Dramatically Stabilize Protein Structure. ACS Chemical Biology, 2019, 14, 1150-1153. | 3.4 | 15 |
| 87 | Harnessing the power of an X-ray laser for serial crystallography of membrane proteins crystallized in lipidic cubic phase. IUCrJ, 2020, 7, 976-984. | 2.2 | 15 |
| 88 | Crystal structure of an alanine-glyoxylate aminotransferase from Anabaena sp. at 1.70 Ã resolution reveals a noncovalently linked PLP cofactor. Proteins: Structure, Function and Bioinformatics, 2005, 58, 971-975. | 2.6 | 14 |
| 89 | Crystal structure of an indigoidine synthase A (IndA)-like protein (TM1464) from Thermotoga maritima at 1.90 Å resolution reveals a new fold. Proteins: Structure, Function and Bioinformatics, 2005, 59, 864-868. | 2.6 | 13 |
| 90 | Crystal structure of Hsp33 chaperone (TM1394) from Thermotoga maritima at 2.20 Ã resolution. Proteins: Structure, Function and Bioinformatics, 2005, 61, 669-673. | 2.6 | 13 |

| # | Article | IF | CITATIONS |
|-----|--|------|-----------|
| 91 | Crystal structure of homoserine O-succinyltransferase from Bacillus cereus at 2.4 Ã resolution. Proteins: Structure, Function and Bioinformatics, 2007, 68, 999-1005. | 2.6 | 13 |
| 92 | Crystal Structure of Histidine Phosphotransfer Protein ShpA, an Essential Regulator of Stalk Biogenesis in Caulobacter crescentus. Journal of Molecular Biology, 2009, 390, 686-698. | 4.2 | 13 |
| 93 | Structural insights on ligand recognition at the human leukotriene B4 receptor 1. Nature Communications, 2021, 12, 2971. | 12.8 | 13 |
| 94 | Crystal structure of an Apo mRNA decapping enzyme (DcpS) from Mouse at 1.83 Ã resolution. Proteins: Structure, Function and Bioinformatics, 2005, 60, 797-802. | 2.6 | 12 |
| 95 | The crystal structure of a bacterial Sufuâ€like protein defines a novel group of bacterial proteins that are similar to the Nâ€terminal domain of human Sufu. Protein Science, 2010, 19, 2131-2140. | 7.6 | 12 |
| 96 | Crystal structure of an α/β serine hydrolase (YDR428C) from Saccharomyces cerevisiae at 1.85 Ã resolution. Proteins: Structure, Function and Bioinformatics, 2004, 58, 755-758. | 2.6 | 11 |
| 97 | Crystal structure of NMA1982 from <i>Neisseria meningitidis</i> at 1.5 Ã resolution provides a structural scaffold for nonclassical, eukaryoticâ€ike phosphatases. Proteins: Structure, Function and Bioinformatics, 2007, 69, 415-421. | 2.6 | 11 |
| 98 | Crystal structure of a metalâ€dependent phosphoesterase (YP_910028.1) from <i>Bifidobacterium adolescentis</i> : Computational prediction and experimental validation of phosphoesterase activity. Proteins: Structure, Function and Bioinformatics, 2011, 79, 2146-2160. | 2.6 | 11 |
| 99 | Crystal structure of a putative modulator of DNA gyrase (pmbA) from Thermotoga maritima at 1.95 Ã resolution reveals a new fold. Proteins: Structure, Function and Bioinformatics, 2005, 61, 444-448. | 2.6 | 10 |
| 100 | Crystal structure of the ApbE protein (TM1553) from Thermotoga maritima at 1.58 Ã resolution. Proteins: Structure, Function and Bioinformatics, 2006, 64, 1083-1090. | 2.6 | 10 |
| 101 | An orthogonal seryl-tRNA synthetase/tRNA pair for noncanonical amino acid mutagenesis in Escherichia coli. Bioorganic and Medicinal Chemistry, 2020, 28, 115662. | 3.0 | 10 |
| 102 | Crystal structure of a conserved hypothetical protein (gi: 13879369) from Mouse at 1.90 Å resolution reveals a new fold. Proteins: Structure, Function and Bioinformatics, 2005, 61, 1132-1136. | 2.6 | 9 |
| 103 | Direct-methods determination of an RNA/DNA hybrid decamer at 1.15â€Ã resolution. Acta Crystallographica Section D: Biological Crystallography, 2001, 57, 213-218. | 2.5 | 8 |
| 104 | Comparative structural analysis of a novel glutathioneS-transferase (ATU5508) fromAgrobacterium tumefaciensat 2.0 Ã resolution. Proteins: Structure, Function and Bioinformatics, 2006, 65, 527-537. | 2.6 | 8 |
| 105 | Crystal structure of a novel archaeal AAA+ ATPase SSO1545 from <i>Sulfolobus solfataricus</i> . Proteins: Structure, Function and Bioinformatics, 2009, 74, 1041-1049. | 2.6 | 8 |
| 106 | Crystal structure of phosphoribosylformylglycinamidine synthase II (smPurL) from Thermotoga maritima at 2.15 A resolution. Proteins: Structure, Function and Bioinformatics, 2006, 63, 1106-1111. | 2.6 | 7 |
| 107 | Crystal structure of an ORFan protein (TM1622) fromThermotoga maritimaat 1.75 Ã resolution reveals a fold similar to the Ran-binding protein Mog1p. Proteins: Structure, Function and Bioinformatics, 2006, 65, 777-782. | 2.6 | 7 |
| 108 | Crystal structure of AICAR transformylase IMP cyclohydrolase (TM1249) from <i>Thermotoga maritima</i> at 1.88 Ã resolution. Proteins: Structure, Function and Bioinformatics, 2008, 71, 1042-1049. | 2.6 | 7 |

| # | Article | IF | CITATIONS |
|-----|---|------------------|-----------|
| 109 | Crystal structure of virulence factor CJ0248 from Campylobacter jejuni at 2.25 Ã resolution reveals a new fold. Proteins: Structure, Function and Bioinformatics, 2005, 62, 292-296. | 2.6 | 6 |
| 110 | Crystal structure of TM1367 from Thermotoga maritima at 1.90 Ã resolution reveals an atypical member of the cyclophilin (peptidylprolyl isomerase) fold. Proteins: Structure, Function and Bioinformatics, 2006, 63, 1112-1118. | 2.6 | 6 |
| 111 | Crystal structure of MtnX phosphatase from <i>Bacillus subtilis</i> at 2.0 à resolution provides a structural basis for bipartite phosphomonoester hydrolysis of 2â€hydroxyâ€3â€ketoâ€5â€methylthiopentenylâ€1â€phosphate. Proteins: Structure, Function and Bioinformatic 2007. 69. 433-439. | s ^{2.6} | 6 |
| 112 | Crystal structure of an ADPâ€ribosylated protein with a cytidine deaminaseâ€like fold, but unknown function (TM1506), from <i>Thermotoga maritima</i> at 2.70 Ã resolution. Proteins: Structure, Function and Bioinformatics, 2008, 71, 1546-1552. | 2.6 | 6 |
| 113 | Crystal structure of TM1030 from Thermotoga maritima at 2.3 Ã resolution reveals molecular details of its transcription repressor function. Proteins: Structure, Function and Bioinformatics, 2007, 68, 418-424. | 2.6 | 5 |
| 114 | Crystal structures of MW1337R and lin2004: Representatives of a novel protein family that adopt a fourâ€helical bundle fold. Proteins: Structure, Function and Bioinformatics, 2008, 71, 1589-1596. | 2.6 | 3 |
| 115 | Lactate dehydrogenase from the hyperthermophilic archaeon Methanococcus jannaschii: overexpression, crystallization and preliminary X-ray analysis. Acta Crystallographica Section D: Biological Crystallography, 2000, 56, 81-83. | 2.5 | 2 |
| 116 | Advances in Structure Determination of G Protein-Coupled Receptors by SFX. , 2018, , 301-329. | | 2 |
| 117 | Crystal structure of a voltage-gated K+ channel pore module in a closed state in lipid membranes Journal of Biological Chemistry, 2013, 288, 3476. | 3.4 | 0 |
| 118 | Allosteric Coupling of Drug Binding and Intracellular Signaling in the A2A Adenosine Receptor. , 2021, , 184-196. | | 0 |